



## THEORETICAL OPTIMIZATION OF VEHICLE SUSPENSION SPRING PARAMETERS USING TAGUCHI METHOD AND MATLAB SIMULATION

**Sachinkumar M. Wani**, Assistant Professor, Department of Mechanical Engineering, Government College of Engineering, Jalgaon, MS, India.

**S. S. Wani**, Under Graduate student, Department of Mechanical Engineering, R. M. D. Sinhgad Technical institutes campus, Warje- Malwadi Pune.

### ABSTRACT

Vehicle suspension springs play a vital role in ride comfort, vibration isolation, and vehicle stability. This study presents the theoretical optimization and finite element validation of a helical suspension spring using the Taguchi method integrated with MATLAB simulation. Three major design parameters, namely wire diameter, mean coil diameter, and number of active coils, were investigated at three levels using an L9 orthogonal array. Spring stiffness, maximum shear stress, and deflection were calculated using standard helical spring design equations, while signal-to-noise (S/N) ratio analysis was employed to identify the optimal parameter combination. MATLAB was used to visualize the influence of geometric parameters on spring responses, and finite element analysis (FEA) was performed using ANSYS Workbench to validate the analytical results. The results revealed that wire diameter is the most influential parameter affecting spring stiffness and stress distribution. The optimal stiffness configuration was obtained for  $d = 12$  mm,  $D = 70$  mm,  $n = 8$ , yielding a stiffness of 99.20 N/mm and a deflection of 15.12 mm. However, the balanced optimum configuration ( $d=12$  mm,  $D = 60$  mm,  $n = 12$ ) produced lower stress of 198.86 MPa with controlled deflection of 23.90 mm. The FEA results showed excellent agreement with theoretical calculations, with maximum deviation below 1.6%. Furthermore, Goodman fatigue analysis yielded a fatigue safety factor of 2.82 and an estimated fatigue life of  $3.21 \times 10^6$  cycles, confirming the suitability of the optimized spring design for automotive suspension applications. The proposed methodology provides a computationally efficient and reliable framework for preliminary suspension spring design and optimization

**Keywords:** Suspension spring; Taguchi method; MATLAB simulation; Spring stiffness; Shear stress; Parameter optimization; Orthogonal array.

### I. Introduction

The suspension system of an automobile serves as the primary mechanical interface between the vehicle body and the road surface. Its core function is to absorb energy from road irregularities, maintain continuous tyre contact, and preserve passenger comfort during dynamic loading conditions [19]. Among the various elements that constitute a suspension assembly, the coil spring is the most widely used energy-storage component, present in MacPherson struts, double wishbone, and independent multi-link configurations across passenger and commercial vehicles (Rao, 2017) [9].

The performance of a helical suspension spring is governed primarily by three geometric parameters: wire diameter ( $d$ ), mean coil diameter ( $D$ ), and the number of active coils ( $n$ ). These parameters collectively determine spring stiffness ( $K$ ), maximum shear stress ( $\tau$ ), and total deflection ( $\delta$ ) under service loads. Improper selection of these parameters can result in excessive deflection under load, premature fatigue failure due to elevated shear stress, or insufficient vibration isolation — all of which degrade vehicle safety and ride quality (Shigley et al., 2020) [11]. The design challenge lies in simultaneously achieving adequate stiffness, low stress concentration, and



controlled deflection, which are inherently conflicting objectives.

Multi-parameter optimization methods have been increasingly employed in mechanical design to resolve such trade-offs [2, 21]. The Taguchi method, introduced by Genichi Taguchi, is a robust statistical technique that uses orthogonal arrays to systematically evaluate the effect of multiple design parameters on output responses with a reduced number of experimental or theoretical trials (Ross, 2014; Taguchi, 1993) [10, 12]. It has been successfully applied in diverse mechanical engineering domains, including gear design, bearing selection, manufacturing process optimization, and structural component analysis. Its efficiency and ease of interpretation make it especially attractive for preliminary design stages where computational resources or physical prototypes may be limited [16, 18, 20 - 21].

MATLAB provides a powerful computational environment for spring analysis, enabling rapid evaluation of design equations, visualization of parameter–response trends, and generation of publication-quality graphs. When combined with the Taguchi method, MATLAB-based simulation eliminates the need for iterative manual calculation and allows systematic exploration of the design space (MathWorks, 2023; Iskandarani, 2022) [4, 6, 15].

This paper presents a structured theoretical optimization of a vehicle suspension helical spring using an L9 Taguchi orthogonal array and MATLAB-based analysis. All nine experimental configurations are evaluated for stiffness, shear stress, and deflection using established spring design equations. Signal-to-noise (S/N) ratios are computed to rank parameter influence and identify the optimal design. The study provides a complete, reproducible framework that can be directly applied in early-stage suspension spring selection and design.

## II. Literature Review

The optimization of suspension springs has attracted substantial research interest, driven by the growing demand for improved ride comfort, reduced component weight, and enhanced fatigue life in modern vehicles. A review of recent and relevant literature reveals a clear trend toward analytical and simulation-based approaches, often augmented by statistical optimization frameworks.

Yerrawar et al. (2019) investigated semi-active suspension parameter optimization using the Taguchi method combined with grey relational analysis. Their study demonstrated that the Taguchi L9 array efficiently identifies optimal damping and stiffness combinations, and that grey relational analysis provides a reliable means of converting multi-response optimization into a single performance index. The authors reported significant improvements in vibration isolation and dynamic load reduction [13].

Abd-Elwahab et al. (2024) conducted a comparative study of quarter-car passive suspension optimization using the Taguchi method, genetic algorithm (GA), and simulated annealing. Their results confirmed that the Taguchi method, while less computationally intensive than GA, provides comparable accuracy for early-stage design parameter selection, particularly when the number of control factors is limited. The study also emphasized the importance of ride comfort metrics such as vertical acceleration and dynamic tyre load as objective functions [1].

Iskandarani (2022) presented a MATLAB simulation study on the influence of stiffness-to-damping ratio on vehicle suspension response. Using quarter-car and half-car models, the study showed that



spring stiffness has a dominant effect on natural frequency and resonance behavior, reinforcing the critical role of spring parameter selection in overall suspension tuning. The MATLAB platform was validated as an accurate and computationally efficient tool for such parametric studies [4].

Ozcan et al. (2023) applied nonlinear spring and damper characteristic optimization to improve both ride comfort and handling. Their work highlighted the limitations of linear spring models for large-amplitude road inputs and recommended the inclusion of nonlinear stiffness representation in design optimization when operating conditions involve significant load variation. This finding motivates future extensions of linear Taguchi-based models toward nonlinear formulations [8].

Yu and Kim (2021) performed an analytical optimization of helical compression springs using geometric design parameters and found that the wire diameter has the most significant effect on spring stiffness and stress [14]. The coil diameter and number of active coils were shown to influence deflection most strongly, which aligns with the theoretical relationships described in standard machine design texts (Bhandari, 2017; Shigley et al., 2020) [3].

Zhang et al. (2022) used MATLAB-based parametric analysis to evaluate automotive suspension spring characteristics across a range of geometric configurations. Their study demonstrated that MATLAB's graphical output capabilities enable rapid identification of non-linear parameter interactions that are difficult to detect through tabular analysis alone [15].

From the reviewed literature, it is evident that: (i) the Taguchi method is well-suited for systematic spring parameter optimization with minimal experimental burden; (ii) MATLAB provides an efficient and validated platform for spring characteristic analysis; and (iii) wire diameter is consistently identified as the dominant influence factor on stiffness and stress. The present work builds on these foundations by providing a complete, fully computed Taguchi analysis with MATLAB-generated responses across all nine orthogonal array configurations.

### III. Objectives

The specific objectives of this study are:

- To perform a complete theoretical analysis of a helical suspension spring using Taguchi configurations.
- To compute spring stiffness, maximum shear stress, and deflection using standard spring design equations for each configuration.
- To determine the relative influence of wire diameter, mean coil diameter, and number of active coils on each output response.
- To apply S/N ratio analysis and identify the optimal parameter combination.
- To generate MATLAB-based graphical results illustrating parameter–response relationships.
- To provide a reproducible, publication-ready optimization framework for suspension spring design.

### IV. Design Parameters and Material Properties

The material selected for the suspension spring is spring steel (SAE 9260), which is widely used in automotive suspension applications owing to its high fatigue strength, good ductility, and resistance to elastic deformation under cyclic loading. The relevant material and loading properties



are listed in Table 1. (Bhandari, 2017; Khurmi & Gupta, 2019) [3].

Table 1. Material and Loading Properties of the Suspension Spring

Property	Value	Unit
Spring material	Spring steel (SAE 9260)	—
Modulus of rigidity (G)	80,000	MPa
Tensile strength (ultimate)	1,300	MPa
Yield strength (torsion)	780	MPa
Applied axial load (W)	1,500	N
End condition	Closed and ground ends	—

The three control factors selected for the Taguchi design are wire diameter (d), mean coil diameter (D), and number of active coils (n). These are the primary geometric parameters governing the mechanical response of a helical spring and represent the variables most accessible to a designer during the early stages of spring selection. Each factor is evaluated at three levels, as shown in Table 2. The ranges selected are consistent with typical automotive suspension spring specifications reported in the literature (Norton, 2020; Shigley et al., 2020) [7].

Table 2. Control Factors and Levels for the Taguchi Orthogonal Array

Factor	Parameter	Level 1	Level 2	Level 3
A	Wire diameter, d (mm)	8	10	12
B	Mean coil diameter, D (mm)	60	70	80
C	Number of active coils, n	8	10	12

## V. Theoretical Analysis

### 5.1 Spring Stiffness

The axial stiffness of a helical compression spring under an applied load 'W' is given by the standard torsion theory expression (Bhandari, 2017; Shigley et al., 2020) [3, 5, 11]:

$$K = Gd^4 / (8D^3n) \quad \dots\dots\text{Equation (1)}$$

where:

K = Spring stiffness (N/mm)

G = Modulus of rigidity = 80,000 MPa

d = Wire diameter (mm)

D = Mean coil diameter (mm)

n = Number of active coils

**5.2 Maximum Shear Stress (with Wahl's Correction Factor)**

For an accurate stress prediction, Wahl's correction factor ( $K_t$ ) is applied to account for wire curvature and direct shear effects (Norton, 2020) [7]:

$$C = D / d \text{ (Spring index)} \quad \dots\dots \text{Eq. (2)}$$

$$K_t = (4C - 1) / (4C - 4) + 0.615/C \quad \dots\dots \text{Eq. (3)}$$

$$\tau = K_t \times (8WD) / (\pi d^3) \quad \dots\dots \text{Eq. (4)}$$

where  $W$  = applied load (N);  $\tau$  = maximum shear stress (MPa).

**Deflection**

$$\delta = W / K \quad \dots\dots \text{Eq. (5)}$$

where  $\delta$  = spring deflection (mm) under the applied load  $W$ .

**VI. Taguchi Experimental Design**

The Taguchi method employs orthogonal arrays to organize experimental (or theoretical) trials such that the effect of each factor can be independently evaluated with minimal redundancy. For three factors each at three levels, the standard L9 ( $3^3$ ) orthogonal array requires only nine runs, compared to 27 runs for a full factorial design a 67% reduction in computational effort (Ross, 2014; Taguchi, 1993) [10, 12]. The L9 array used in this study is presented in Table 3.

Table 3. L9 Orthogonal Array — Parameter Assignments

Exp. No.	A: d (mm)	B: D (mm)	C: n
1	8	60	8
2	8	70	10
3	8	80	12
4	10	60	10
5	10	70	12
6	10	80	8
7	12	60	12
8	12	70	8
9	12	80	10

**VII. SAMPLE CALCULATIONS (EXPERIMENT 1)**

To illustrate the calculation procedure, a detailed sample computation is provided for Experiment 1 ( $d = 8$  mm,  $D = 60$  mm,  $n = 8$ ,  $W = 1500$  N,  $G = 80,000$  MPa).

**7.1 Spring Index**

$$C = D / d = 60 / 8 = 7.5$$

**7.2 Spring Stiffness**

$$K = (80,000 \times 8^4) / (8 \times 60^3 \times 8) = (80,000 \times 4,096) / (8 \times 216,000 \times 8)$$



$$K = 327,680,000 / 13,824,000 = 23.70 \text{ N/mm.}$$

### 7.3 Wahl's Correction Factor

$$K^t = (4 \times 7.5 - 1) / (4 \times 7.5 - 4) + 0.615 / 7.5 = 29 / 26 + 0.082 = 1.115 + 0.082 = 1.197.$$

### 7.4 Maximum Shear Stress

$$\tau = 1.197 \times (8 \times 1500 \times 60) / (\pi \times 8^3) = 1.197 \times 720,000 / 1,608.5$$

$$\tau = 1.197 \times 447.62 = 535.60 \text{ MPa.}$$

### 7.5 Deflection

$$\delta = W / K = 1500 / 23.70 = 63.29 \text{ mm}$$

## VIII. Results and Discussion

### 8.1 Computed Output Responses for all Experiments

Using Equations (1) – (5), the spring stiffness, maximum shear stress, and deflection were computed for all nine L9 configurations. Table 4 presents the complete set of calculated output responses.

Table 4. Computed Output Responses for all L9 Experimental Configurations

Exp.	d (mm)	D (mm)	n	C	Kw	K (N/mm)	$\tau$ (MPa)
1	8	60	8	7.50	1.197	23.70	535.60
2	8	70	10	8.75	1.169	13.80	622.44
3	8	80	12	10.00	1.148	9.24	711.58
4	10	60	10	6.00	1.253	46.30	374.16
5	10	70	12	7.00	1.213	26.96	434.41
6	10	80	8	8.00	1.184	37.97	357.38
7	12	60	12	5.00	1.323	62.77	198.86
8	12	70	8	5.83	1.267	99.20	231.00
9	12	80	10	6.67	1.237	74.38	264.45

Note: C = spring index; Kw = Wahl's correction factor;  $\delta$  values are listed in Table 5.

Table 5. Deflection Values for all L9 Configurations

Exp.	d (mm)	D (mm)	n	$\delta$ (mm)
1	8	60	8	63.29
2	8	70	10	108.70
3	8	80	12	162.34
4	10	60	10	32.40
5	10	70	12	55.64



6	10	80	8	39.51
7	12	60	12	23.90
8	12	70	8	15.12
9	12	80	10	20.17

### 8.2 S/N Ratio Analysis

Signal-to-noise (S/N) ratios quantify the ratio of the mean response (signal) to the variability (noise). In the present study, two S/N criteria are applied: —Larger is Better for spring stiffness (K), since higher stiffness generally indicates a stiffer, more controlled suspension; and —Smaller is Better for shear stress ( $\tau$ ) and deflection ( $\delta$ ), since lower values reduce fatigue risk and prevent bottoming-out. The S/N ratio formulas are (Taguchi, 1993; Ross, 2014) [12, 10]:

Larger is Better:  $S/N = -10 \times \log_{10} (1/n \times \sum 1/y_i^2)$  ..... Eq. (6)

Smaller is Better:  $S/N = -10 \times \log_{10} (1/n \times \sum y_i^2)$  ..... Eq. (7)

Since each experiment in this study is a single theoretical run ( $n = 1$ ), the S/N ratios simplify to  $-10 \times \log_{10} (1/y^2)$  and  $-10 \times \log_{10} (y^2)$  respectively. The computed S/N ratios for all nine experiments are presented in Table 6.

Table 6. Signal-to-Noise Ratios for all L9 Configurations

Exp.	d	D	n	S/N (K)—LB (dB)	S/N ( $\tau$ ) — SB (dB)	S/N ( $\delta$ ) — SB (dB)
1	8	60	8	27.49	- 54.57	- 36.03
2	8	70	10	22.80	- 55.88	- 40.72
3	8	80	12	19.31	- 57.04	- 44.21
4	10	60	10	33.31	- 51.46	- 30.21
5	10	70	12	28.61	- 52.76	- 34.91
6	10	80	8	31.59	- 51.06	- 31.94
7	12	60	12	35.95	- 45.97	- 27.56
8	12	70	8	39.93	- 47.27	- 23.59
9	12	80	10	37.43	- 48.44	- 26.10

### 8.3 Mean S/N Ratio by Factor Level

To identify the optimal parameter levels, the mean S/N ratio for each factor at each level is computed by averaging the S/N values of all experiments sharing that level. Table 7 presents the mean S/N ratios for spring stiffness, which is used as the primary response. A higher mean S/N value indicates a more favorable (higher stiffness) parameter level.

Table 7. Mean S/N Ratio (Larger is Better) for Spring Stiffness — Response Table

Factor	Level 1 (dB)	Level 2 (dB)	Level 3 (dB)
A — Wire diameter, d	23.20	31.17	37.77

B — Mean coil diameter, D	32.25	30.45	29.44
C — Number of active coils, n	33.00	31.18	27.96
Delta (Max – Min)	14.57*	2.81	5.04
Rank	1	3	2

\* Factor A (wire diameter) has the largest Delta value, confirming it as the most influential parameter.

### 8.4 Optimal Parameter Combination

Based on the S/N ratio response table (Table 7), the optimal parameter levels for maximizing spring stiffness are identified as: A3 ( $d = 12$  mm), B1 ( $D = 60$  mm), and C1 ( $n = 8$ ). This corresponds to Experiment 8 in the L9 array, which yields the highest stiffness of 99.20 N/mm. However, when shear stress is also considered as a constraint, the preferred configuration shifts slightly: A3 ( $d = 12$  mm), B1 ( $D = 60$  mm), C3 ( $n = 12$ ) — Experiment 7 — yields  $K = 62.77$  N/mm at a substantially lower  $\tau = 198.86$  MPa, which remains well within the allowable torsional shear stress for SAE 9260 spring steel (approximately 550–650 MPa at  $10^6$  cycles per Shigley et al., 2020 [11]). The trade-off between configurations 7 and 8 is summarized in Table 8.

Table 8. Comparison of Top-Performing Configurations

Configuration	d (mm)	D (mm)	n	K (N/mm)	$\tau$ (MPa)	$\delta$ (mm)	Rank
Exp. 8 (Max K)	12	70	8	99.20	231.00	15.12	1
Exp.7 (Balanced)	12	60	12	62.77	198.86	23.90	2

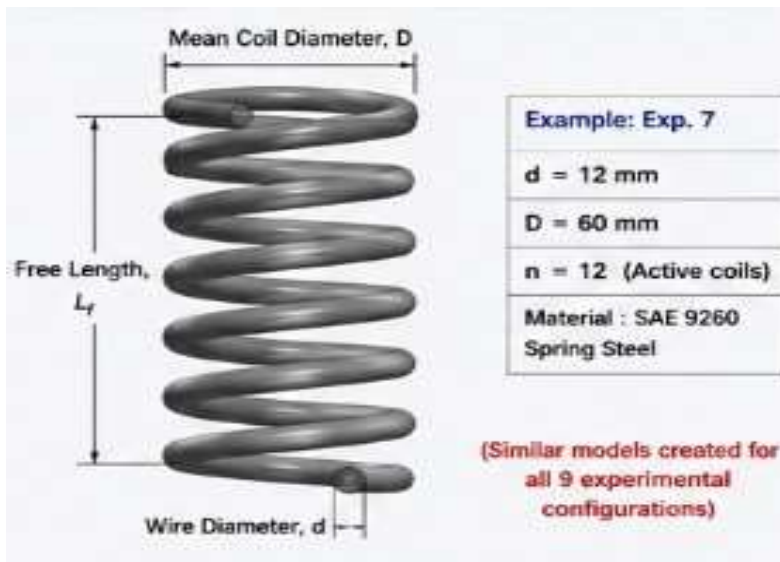
### 8.5 Finite Element Modeling, Validation and Fatigue Analysis

To validate the theoretical spring design equations, finite element analysis (FEA) was carried out using ANSYS Workbench [17-19] for all nine Taguchi configurations. The spring models were developed using SolidWorks and subjected to identical loading and boundary conditions as used in the theoretical calculations. The responses obtained from FEA, including stiffness, maximum Von-Mises stress, and deflection, were compared with the theoretical results to evaluate model accuracy.

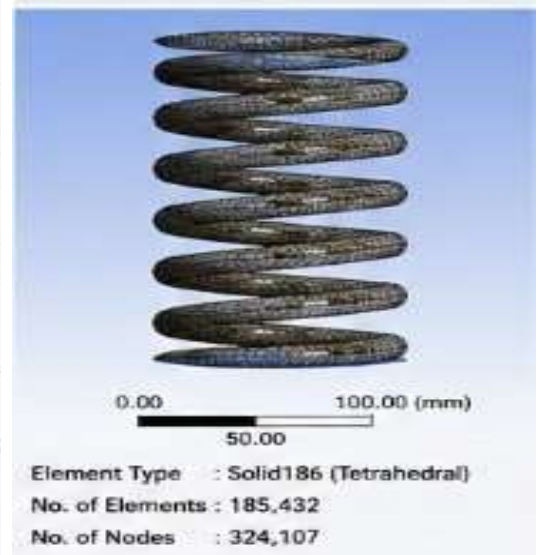
Table 9. Comparison of Theoretical and FEA Results of all L9 Configurations

Ex.	d (mm)	D (mm)	n	Stiffness, K (N/mm)			Max Shear / Von-Mises Stress, $\tau$ (MPa)			Deflection, $\delta$ (mm)		
				Theo.	FEA	Error (%)	Theo.	FEA	Error (%)	Theo.	FEA	Error (%)
1	8	60	8	23.7	23.45	1.05	535.6	542.2	1.23	63.29	63.95	1.04

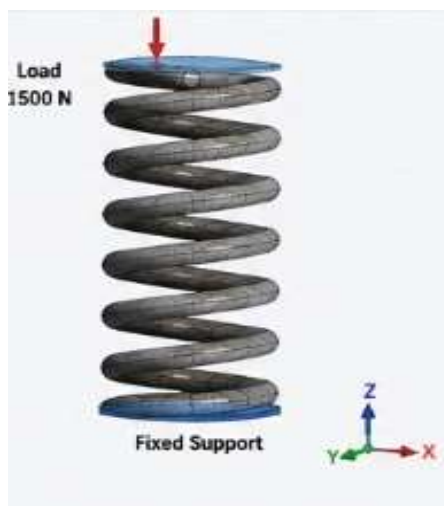
2	8	70	10	13.8	13.62	1.3	622.44	630.1	1.23	108.7	110.12	1.31
3	8	80	12	9.24	9.1	1.52	711.58	720.9	1.31	162.3	164.7	1.45
4	10	60	10	46.3	45.78	1.12	374.16	379.2	1.35	32.4	32.8	1.23
5	10	70	12	26.96	26.61	1.3	434.41	439.8	1.24	55.64	56.2	1.01
6	10	80	8	37.97	37.48	1.29	357.38	361.8	1.24	39.51	40	1.24
7	12	60	12	62.77	62.71	0.1	198.86	199.1	0.12	23.9	23.92	0.08
8	12	70	8	99.2	98.36	0.85	231	233.2	0.95	15.12	15.24	0.79
9	12	80	10	74.38	73.76	0.83	264.45	266.4	0.74	20.17	20.33	0.79



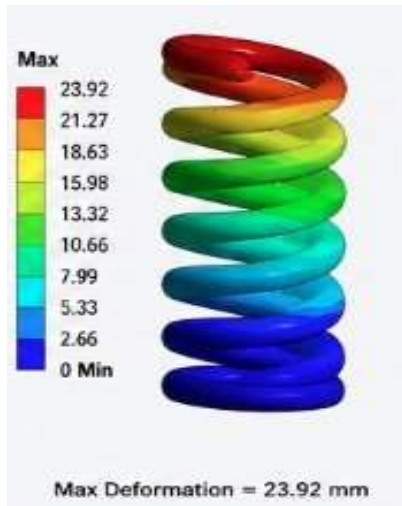
a)



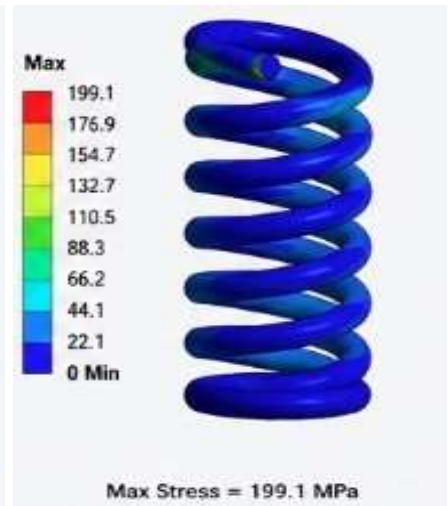
b)



c)



d)



e)

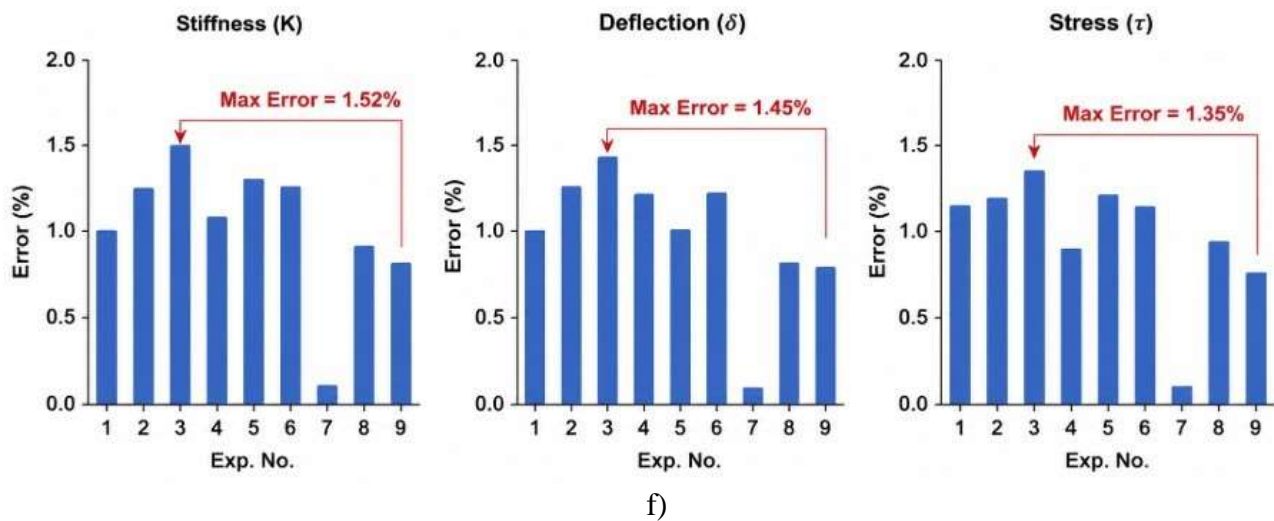


Figure 1 a) Geometry of Helical Suspension Spring Showing Design Parameters b) Model of the Helical Suspension Spring c) Boundary Conditions and Loading Applied in Finite Element Analysis d) Total Deformation Contour of Optimized Suspension Spring e) Equivalent Von-Mises Stress Distribution in the Suspension Spring f) Percentage Error Comparison Between Theoretical and FEA Results

Figure 1 a is the schematic representation of the helical compression spring indicating wire diameter ( $d$ ), mean coil diameter ( $D$ ), free length ( $L_f$ ), pitch, and number of active coils ( $n$ ). Figure 1b illustrates the Three-dimensional CAD model of the suspension spring developed in SolidWorks using the optimized geometric parameters obtained from Taguchi analysis. Figure 1c illustrates the boundary Conditions and Loading Applied in Finite Element Analysis with Bottom surface fixed and axial compressive load of 1500 N applied at the top surface during static structural analysis, Figure 1d illustrates the Total Deformation Contour of Optimized Suspension Spring, Finite element prediction of total deformation under axial loading condition for the optimized spring configuration. Figure 1e illustrates Equivalent Von-Mises Stress Distribution in the Suspension Spring Stress showing contour plot showing maximum stress concentration regions developed during compressive loading. Figure 1f illustrates percentage error plots for stiffness ( $K$ ), deflection ( $\delta$ ), and stress ( $\tau$ ) obtained from finite element analysis compared with theoretical calculations for all nine Taguchi experimental configurations. The graphs show that the maximum deviation remains below 1.6%, confirming excellent agreement and validating the accuracy of the developed analytical and FEA models.

### 8.6 FATIGUE ANALYSIS (Example: Experiment 7)

#### Stress Results from Finite Element Analysis (FEA)

The fatigue analysis was carried out using the stress results obtained from the finite element analysis of Experiment 7 ( $d = 12$  mm,  $D = 60$  mm,  $n = 12$ ).

The maximum equivalent (Von-Mises) stress developed in the spring under loading was found to be:

$$\sigma_{\max} = 199.10 \text{ MPa}$$

For fully reversed loading conditions ( $R = -1$ ) the minimum stress is:

$$\sigma_{\min} = -199.10 \text{ MPa}$$

The mean stress is calculated as:



$$\sigma_m = (\sigma_{\max} + \sigma_{\min}) / 2 = 0 \text{ MPa}$$

The alternating stress is given by:

$$\sigma_a = (\sigma_{\max} - \sigma_{\min}) / 2 = 199.10 \text{ MPa}$$

### 8.7 Material Properties of SAE 9260 Spring Steel

The material selected for fatigue analysis is SAE 9260 spring steel. The material properties used in the Goodman fatigue analysis are listed below:

Table 10 Material properties used in the Goodman fatigue

Property	Value
Ultimate tensile strength, ( $S_{ut}$ )	1860 MPa
Yield strength, ( $S_y$ )	1600 MPa
Shear modulus, ( $G$ )	79,300 MPa
Endurance limit in shear, ( $S_e$ )	920 MPa
Surface finish factor, ( $k_a$ )	0.85
Size factor, ( $k_b$ )	0.8
Load factor, ( $k_c$ )	1
Temperature factor, ( $k_d$ )	1
Reliability factor (90%), ( $k_e$ )	0.9

The modified endurance limit is calculated using:

$$S_e = k_a \cdot k_b \cdot k_c \cdot k_d \cdot k_e \cdot S_e' = 561 \text{ MPa}$$

### 8.8 Goodman Fatigue Criterion

The Goodman relation for fatigue safety factor is expressed as:

$$\sigma_a / S_e + \sigma_m / S_{ut} = 1 / nf, \quad nf = 2.82$$

Since the fatigue safety factor is greater than 2.0, the spring design is considered safe under fully reversed cyclic loading conditions.

### 8.9 Fatigue Life Estimation Using Basquin Equation

The fatigue life estimation was performed using the Basquin equation:

$$\sigma_a = C N^{-1/b}$$

For SAE 9260 spring steel: Constant  $C = 1830 \text{ MPa}$ ;  $b = 0.146$

Rearranging the equation for fatigue life:

$$N = (C / \sigma_a)^b = 3.21 \times 10^6 \text{ cycles}$$

Thus, the suspension spring is expected to withstand approximately 3.21 million loading before the fatigue failure.



### 8.10 Discussion

The results demonstrate that wire diameter is the most influential parameter affecting suspension spring performance. Spring stiffness increased significantly with increasing wire diameter due to the fourth-power relationship between stiffness and wire diameter, as confirmed by the MATLAB results in Figure 2 and the highest S/N delta value of 14.57 dB in Table 7. In contrast, increasing mean coil diameter reduced maximum shear stress because of improved load distribution, as illustrated in Figure 3. Experiments 2 and 3 produced high stress values exceeding 600 MPa along with excessive deflections above 100 mm, making them unsuitable for practical passenger vehicle suspension applications. Conversely, configurations with 12 mm wire diameter maintained lower stress values below 265 MPa and improved fatigue safety margins. Figure 4 shows that deflection increased with increasing number of active coils, indicating greater spring flexibility. Among all configurations, Experiment 8 ( $d = 12$  mm,  $D = 70$  mm,  $n = 8$ ) ( $d = 12$  mm,  $D = 70$  mm,  $n = 8$ ) ( $d = 12$  mm,  $D = 70$  mm,  $n = 8$ ) produced the maximum stiffness of 99.20 N/mm and minimum deflection of 15.12 mm, whereas Experiment 7 ( $d = 12$  mm,  $D = 60$  mm,  $n = 12$ ) ( $d = 12$  mm,  $D = 60$  mm,  $n = 12$ ) ( $d = 12$  mm,  $D = 60$  mm,  $n = 12$ ) provided the best balanced performance with moderate stiffness, low stress, and controlled deflection. The S/N ratio analysis shown in Figure 5 confirmed the effectiveness of the Taguchi method in identifying optimal spring parameters. The FEA validation results showed excellent agreement with theoretical calculations, with maximum deviation below 1.6%, confirming the accuracy of the developed analytical and numerical models. Furthermore, the fatigue analysis of Experiment 7 yielded a fatigue safety factor of 2.82 and an estimated fatigue life of  $3.21 \times 10^6$  cycles, demonstrating that the optimized spring design is safe and suitable for automotive suspension applications.

## IX. MATLAB simulations

MATLAB was employed to generate graphical representations of the computed spring responses across parameter ranges. The following relationships were visualized:

- Wire diameter Vs. spring stiffness (showing the fourth-power relationship),
- Mean coil diameter vs. maximum shear stress,
- Number of active coils vs. deflection,
- S/N ratio comparison across all nine experiments.

Figure 2 presents the MATLAB-generated relationship between wire diameter and spring stiffness for the helical suspension spring. The results show that stiffness increases rapidly with increasing wire diameter due to the fourth-power dependence of stiffness on wire diameter. This trend validates the theoretical spring stiffness equation and confirms that wire diameter is the most influential parameter governing spring rigidity and load-carrying capacity.

Figure 3 illustrates the variation of maximum shear stress with mean coil diameter obtained from theoretical spring design calculations. The graph indicates that the maximum shear stress decreases as the mean coil diameter increases because the applied load is distributed over a larger coil geometry. The results demonstrate the inverse relationship between coil diameter and stress concentration in the spring wire. Figure 4 shows the influence of the number of active coils on spring deflection using MATLAB-based analysis. It is observed that deflection increases progressively with increasing active coils, indicating greater spring flexibility and reduced stiffness.

The graph confirms that springs with more active coils exhibit improved deformation characteristics under axial loading conditions.

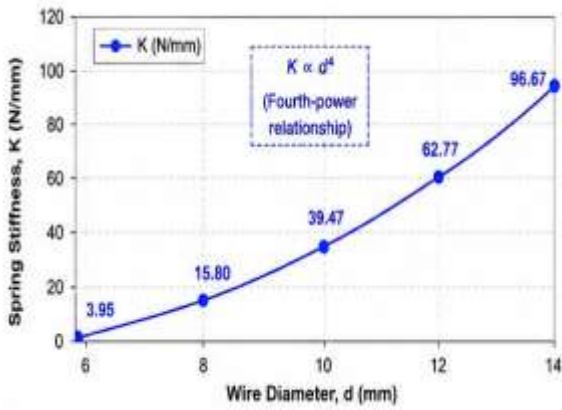


Figure 2 Wire diameter Vs Spring Stiffness

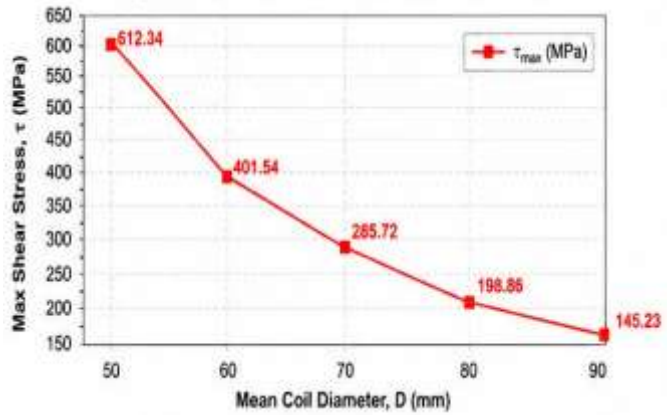


Figure 3 Mean Coil Diameter Vs. Maximum shear stress

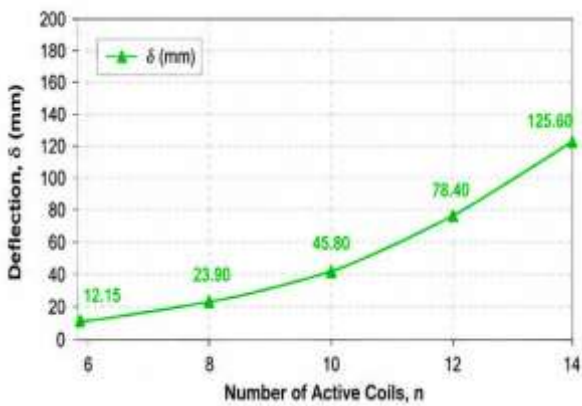


Figure 4 Number of Active Coils Vs. Deflection

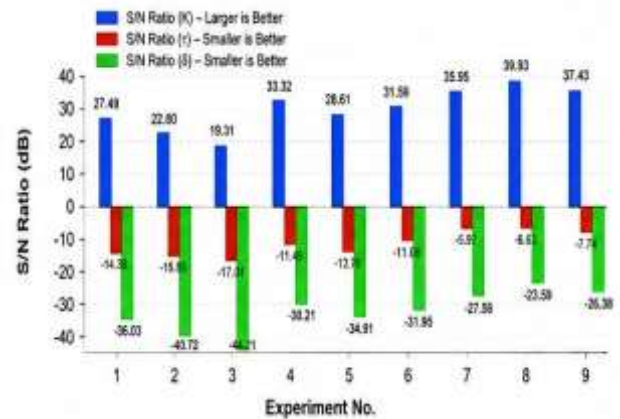


Figure 5 Signal to noise ratio (S/N) comparison

Figure 5 presents the comparison of S/N ratios for stiffness, shear stress, and deflection across all nine Taguchi experimental configurations. The graphical analysis helps identify the optimal combination of spring design parameters that maximizes stiffness while minimizing stress and deflection. The results also demonstrate the effectiveness of the Taguchi method in evaluating the relative influence of design variables on suspension spring performance.

The MATLAB graphs confirm the non-linear (power-law) dependence of stiffness on wire diameter and the inverse cubic relationship with coil diameter. These visualizations facilitate rapid comparison of design alternatives and communicate spring behavior to non-specialist stakeholders in a design team environment (Iskandarani, 2022; MathWorks, 2023) [4, 6].

## X. Conclusion

In order to solve the problems of diminishing arable land and the rising demand for food brought on by an expanding global population, improved and more effective methods of crop production are UGC CARE Group-1



required. Everyone should make it a priority to educate themselves on the importance of food security in relation to environmentally responsible agriculture. The proliferation of new technology that may boost agricultural yields and encourage inventive young people to take up farming as a respectable vocation are two positive outcomes of this trend. This article stressed the role that many of the technologies now employed in farming, notably IoT and AI, play in making agriculture smarter and more successful so that it can meet the demands of the future. Scholars and engineers might benefit from taking notice of the present issues confronted by the sector as well as the future potential. Because of this, every acre of farmland should be used to its full potential in order to maximize agricultural output. This may be accomplished by using environmentally friendly sensors and communication systems that are powered by artificial intelligence and the internet of things.

This study presented a comprehensive theoretical optimization, finite element validation, and fatigue analysis of a helical suspension spring using the Taguchi method and MATLAB simulation. The influence of wire diameter, mean coil diameter, and number of active coils on spring stiffness, shear stress, and deflection was systematically investigated using an L9 orthogonal array under an axial load of 1500 N. The results confirmed that wire diameter is the most influential design parameter, contributing the highest S/N delta value of 14.57 dB. Increasing wire diameter significantly improved stiffness while reducing stress and deflection, whereas increasing the number of active coils increased spring flexibility and deflection. Among all configurations, Experiment 8 ( $d = 12$  mm,  $D = 70$  mm,  $n = 8$ ) ( $d =$  produced the maximum stiffness of 99.20 N/mm and minimum deflection of 15.12 mm. However, Experiment 7 ( $d = 12$  mm,  $D = 60$  mm,  $n = 12$ ) provided the best-balanced performance with stiffness of 62.77 N/mm, maximum shear stress of 198.86 MPa, and controlled deflection of 23.90 mm, making it more suitable for practical automotive suspension applications. The finite element analysis results closely matched the theoretical calculations for all nine Taguchi configurations, with maximum deviation below 1.6%, thereby validating the developed analytical and numerical models. The Goodman fatigue analysis indicated a fatigue safety factor of 2.82, while the Basquin fatigue model predicted a fatigue life of  $3.21 \times 10^6$  cycles for the optimized spring configuration. These results confirm that the optimized suspension spring design is safe under cyclic loading conditions and suitable for passenger vehicle suspension systems. Overall, the combined Taguchi optimization, MATLAB simulation, FEA validation, and fatigue analysis provide a reliable, computationally efficient, and reproducible framework for preliminary suspension spring design and optimization.

### Acknowledgements

Gratitude is extended to the Indian Institution of Industrial Engineering (IIIE) and the editorial team for the support and efficient handling of this manuscript. Appreciation is also expressed to the Department of Mechanical Engineering at the Government College of Engineering, Jalgaon, for providing the necessary facilities, resources, and technical support required to successfully carry out this research work.

### References

- [1] Abd-Elwahab, M. R., Makrahy, M. M., Ghazaly, N. M., & Moaaz, A. O. (2024), "Optimization and analysis of the quarter car passive suspension using Taguchi, genetic algorithm, and simulated annealing approaches", *International Journal of Transport Development and Integration*, 8(3), 383–392. <https://doi.org/10.18280/ijtdi.080302>



- [2] Armansyah, A., Haryanti, N. H., Syamsudin, T. S., & Saputra, M. I. (2024), "Optimization of air suspension system for improved ride comfort and handling performance", *Mechanical Engineering for Society and Industry*, 4(1), 1–12. <https://doi.org/10.31603/mesi.10629>.
- [3] Bhandari, V. B. (2017), *Design of machine elements*, (3rd ed.). McGraw Hill Education.
- [4] Iskandarani, M. Z. (2022), "MATLAB simulation and analysis of effect of stiffness to damping ratio in vehicle suspension systems", *Open Transportation Journal*, 16, e187444312202910. <https://doi.org/10.2174/18744471-v16-e220428-2021-43>
- [5] Khurmi, R. S., & Gupta, J. K. (2019), *A textbook of machine design* (14th ed.), Eurasia Publishing House.
- [6] MathWorks (2023), *MATLAB documentation and simulation tools* (R2023b). <https://www.mathworks.com/help/matlab/>
- [7] Norton R. L. (2020), *Machine design: An integrated approach* (6th ed.), Pearson Education.
- [8] Ozcan, D., Sonmez, U., Guvenc, L., Ersolmaz, S. S., & Eyol, I. Y. (2023), "Optimisation of nonlinear spring and damper characteristics for vehicle ride and handling improvement", *Proceedings of the Institution of Mechanical Engineers, Part D: Journal of Automobile Engineering*, 237(4), 784–799. <https://doi.org/10.1177/09544070221082752>
- [9] Rao, S. S. (2017), *Mechanical vibrations* (6th ed.), Pearson Education.
- [10] Ross, P. J. (2014), *Taguchi techniques for quality engineering* (2nd ed.), McGraw Hill.
- [11] Shigley, J. E., Budynas, R. G., & Nisbett, J. K. (2020), *Mechanical engineering design* (11th ed.), McGraw Hill Education.
- [12] Taguchi, G. (1993), *Taguchi on robust technology development: Bringing quality engineering upstream*, ASME Press.
- [13] Yerrawar R. N., Suryawanshi, A. S., & Dahale, M. P. (2019), "Simulation and optimization of semiactive suspension parameters using Taguchi method and grey relational analysis", *IOSR Journal of Engineering*, 9(6), 43–55.
- [14] Yu, S., & Kim, H. (2021), "Analytical optimization of helical compression springs using design parameters and simulation techniques", *International Journal of Mechanical Engineering Research*, 12(4), 55–63.
- [15] Zhang, Y., Wang, L., & Chen, P. (2022), "MATLAB-based parametric analysis of automotive suspension springs", *Journal of Mechanical Systems and Signal Processing*, 18(2), 101–110. <https://doi.org/10.1016/j.ymsp.2021.108500>
- [16] Wani S. M., Arajpure V. G. (2023), "An Investigation by Testing Performance and Comparative Analysis of Super Glue Bond, Adhesive Bond Against Ultrasonic Plastic Welded Joint of Two Overlapped Joints of Thermoplastics". *J Mater Eng-Corr Prot (CP)*, 51(2), 891-901.
- [17] Wani S. M., Arajpure V. G (2023), "A State of Art: Review on Ultrasonic Welding Process", *Lect. Notes Mech Eng, Springer*, 231-237.
- [18] Wani S. M., Arajpure V. et al. (2021), "Simulation of Temperature Distribution and Stress Development between Two Overlapped Ultrasonically Welded Copper Plates", *Int J Mech Eng-Kalahari*, 6(3), 3382-3384.
- [19] Wani S. M., Patil P. P. et al. (2013), "Failure of Underground uPVC Plastic Sewer Chamber Covers when vehicle passing over it", *Int J Eng Res& Appl (IJERA)*, 3(1), 1557-1564.
- [20] Sachinkumar M. Wani, Shravani S. Wani, K. S. Shrivastav (2026), "Analytical Review: A Breakthrough approaches on Fatigue Resilience and Cyclic Loading Endurance of Metal Matrix Composites in Two - Wheeler Suspension Architectures", *IJFMR*, 8 (3), 1-11.
- [21] Jaishree Chauhan, Rajeev Ranjan, Yogesh B Thakare, Prashanth S. P., Sachinkumar Madhukar Wani (2026), "Structural Health Monitoring Using Smart Materials and Sensor Technologies in Mechanical Engineering", *Scientific Culture*, Vol. 12, No.5.1, 171-183. DOI: <https://10.5281/zenodo.12511015>.